The GPD program in Halls A & C

Carlos Muñoz Camacho

Institut de Physique Nucléaire, CNRS/IN2P3 (France)

June 21, 2018
Joint Hall A and C Summer Meeting

Outline

1. Introduction
2. Nucleon 3D-imaging & Generalized Parton Distributions (GPDs)
3. Deeply Virtual Compton Scattering (DVCS): $ep \rightarrow ep\gamma$
4. Experimental program at Jefferson Lab
   - Recent results on DVCS and π^0 production
   - Experiments at 12 GeV
5. Summary

Studying the structure of the nucleon experimentally

Elastic scattering

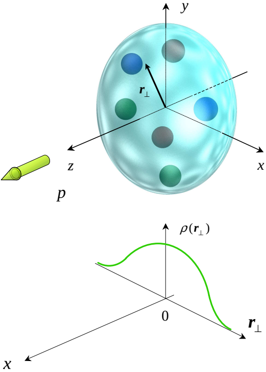

Form factors

Deeply Inelastic Scattering

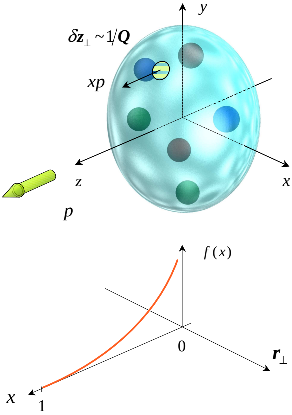

Parton distributions

Hard exclusive processes

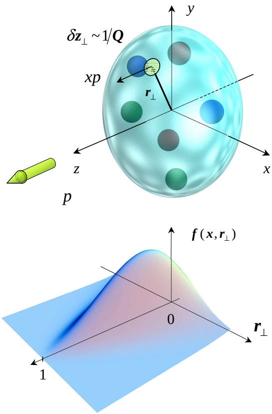

Generalized Parton Distributions (GPDs)

Deeply Virtual Compton Scattering (DVCS): $\gamma^* \, p \to \gamma \, p$

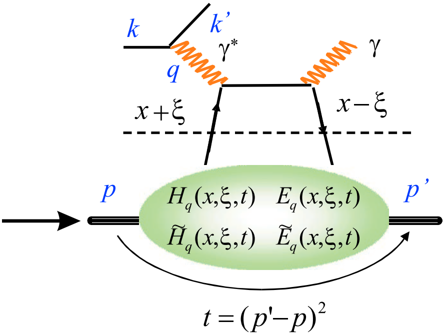

Handbag diagram

High Q^2
Perturbative QCD

Non-perturbative
GPDs

Bjorken limit :

$$\left.\begin{aligned} Q^2 = \quad -q^2 &\to \infty \\ \nu &\to \infty \end{aligned}\right\} \quad x_B = \frac{Q^2}{2M\nu} \text{ fixed}$$

DVCS experimentally: interference with Bethe-Heitler

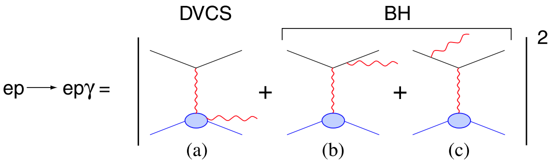

At leading order in $1/Q$ (leading twist) :

$$d^5\overrightarrow{\sigma} - d^5\overleftarrow{\sigma} = \Im m\left(T^{BH}\cdot T^{DVCS}\right)$$

$$d^5\overrightarrow{\sigma} + d^5\overleftarrow{\sigma} = |BH|^2 + \Re e\left(T^{BH}\cdot T^{DVCS}\right) + |DVCS|^2$$

$$\mathcal{T}^{DVCS} = \int_{-1}^{+1} dx \frac{H(x,\xi,t)}{x-\xi+i\epsilon} + \cdots =$$

$$\underbrace{\mathcal{P}\int_{-1}^{+1} dx \frac{H(x,\xi,t)}{x-\xi}}_{\text{Access in helicity-independent cross section}} - \underbrace{i\pi H(x=\xi,\xi,t)}_{\text{Access in helicity-dependent cross-section}} + \ldots$$

Leading twist GPDs

8 GPDs related to the different combination of quark/nucleon helicities

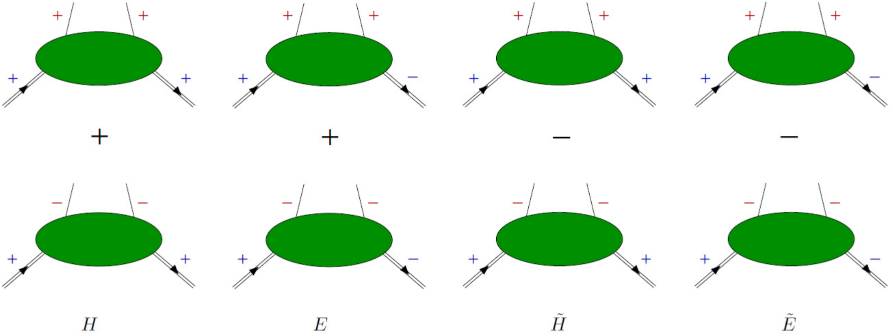

4 chiral-even GPDs: conserve the helicity of the quark

Access through DVCS (and DVMP)

Leading twist GPDs

8 GPDs related to the different combination of quark/nucleon helicities

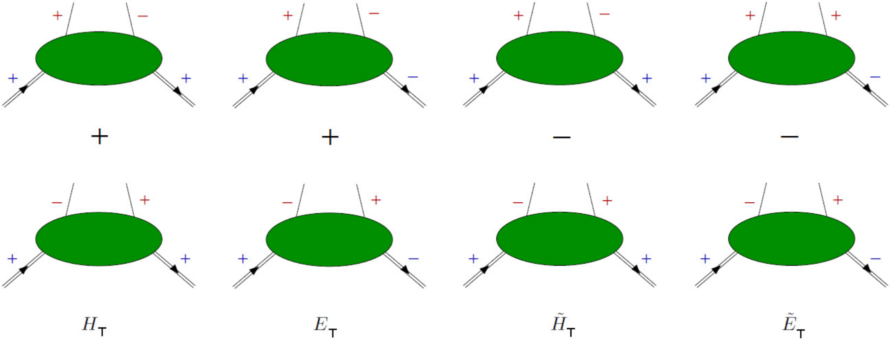

4 chiral-odd GPDs: flip helicity of the quark

"transversity GPDs"

Experimental access more complicated (π^0 electroproduction?)

Kinematic coverage

Kinematic complementarity between different facilities:

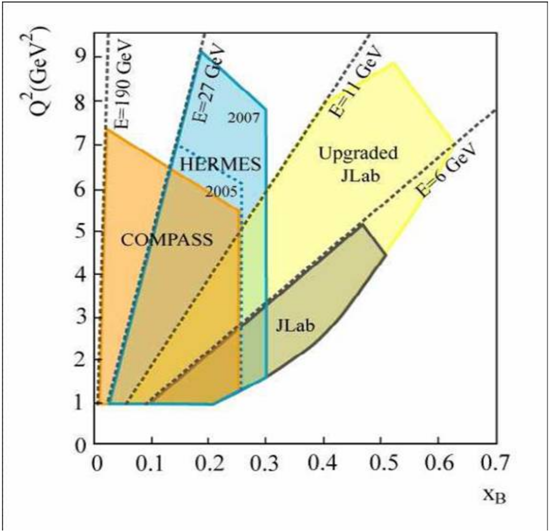

The GPD experimental program at Jefferson Lab

- Hall A: high accuracy, limited kinematic coverage
- Hall B: wide kinematic range, limited precision
- Hall C: high precision program at 11 GeV

Partially overlapping, partially complementary programs
with different experimental setups

The roadmap:

- Early results (2001) from non-dedicated experiment (CLAS)
- 1^{st} round of dedicated experiments in Halls A/B in 2004/5
- 2^{nd} round on 2008–2010: precision tests + more spin observables
- Compeling DVCS experiments in Halls A+B+C at 11 GeV ($\gtrsim$2017)

Experimental setup

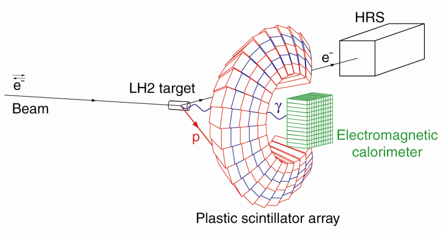

High Resolution Spectrometer

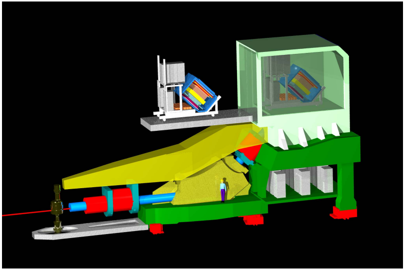

100-channel scintillator array

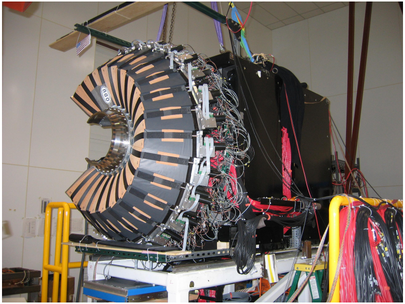

132-block PbF_2 electromagnetic calorimeter

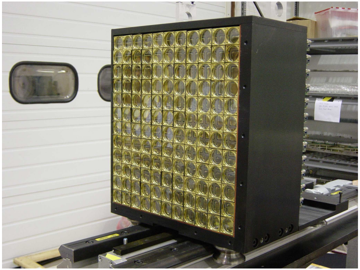

DVCS cross sections: azimuthal analysis

$Q^2 = 2.36\ \text{GeV}^2,\ x_B = 0.37,\ -t = 0.32\ \text{GeV}^2$

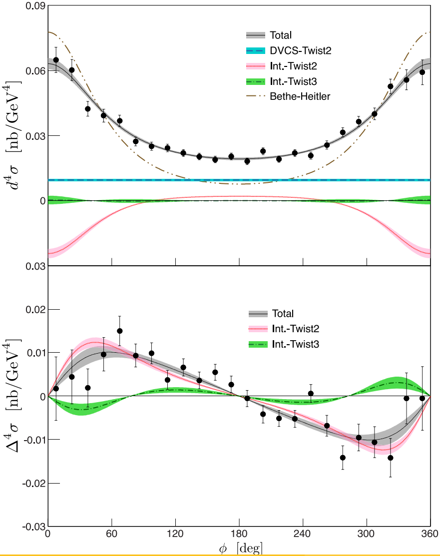

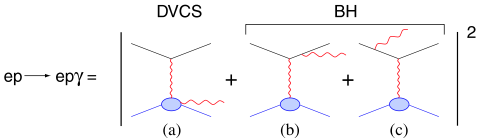

$$d^4\sigma = \mathcal{T}_{\mathsf{BH}}^2 + \mathcal{T}_{\mathsf{BH}}\mathcal{R}e(\mathcal{T}_{\mathsf{DVCS}}) + \mathcal{T}_{\mathsf{DVCS}}^2$$

$$\mathcal{R}e(\mathcal{T}_{\mathsf{DVCS}}) \sim c_0^{\mathcal{I}} + c_1^{\mathcal{I}}\cos\phi + c_2^{\mathcal{I}}\cos 2\phi$$

$$\mathcal{T}_{\mathsf{DVCS}}^2 \sim c_0^{\mathsf{DVCS}} + c_1^{\mathsf{DVCS}}\cos\phi$$

$$\Delta^4\sigma = \frac{d^4\overrightarrow{\sigma} - d^4\overleftarrow{\sigma}}{2} = \mathcal{I}m(\mathcal{T}_{\mathsf{DVCS}})$$

$$\mathcal{I}m(\mathcal{T}_{\mathsf{DVCS}}) \sim s_1^{\mathcal{I}}\sin\phi + s_2^{\mathcal{I}}\sin 2\phi$$

M. Defurne *et al.* Phys. Rev. C 92, 055202

DVCS cross sections: Q^2–dependance

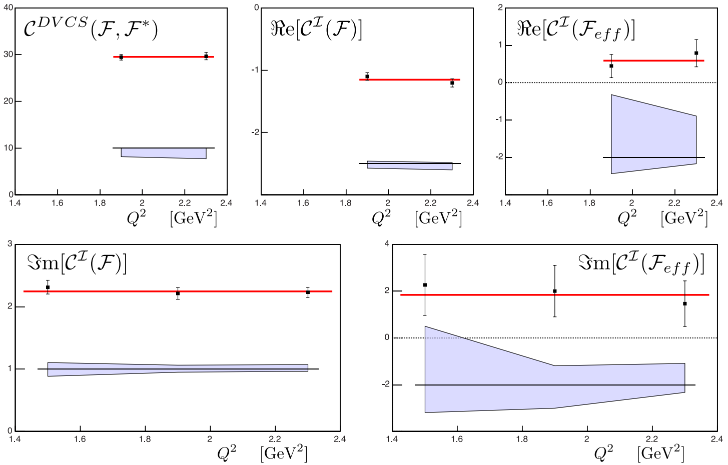

No Q^2-dependance within limited range ⇒ leading twist dominance

DVCS cross sections: kinematical power corrections

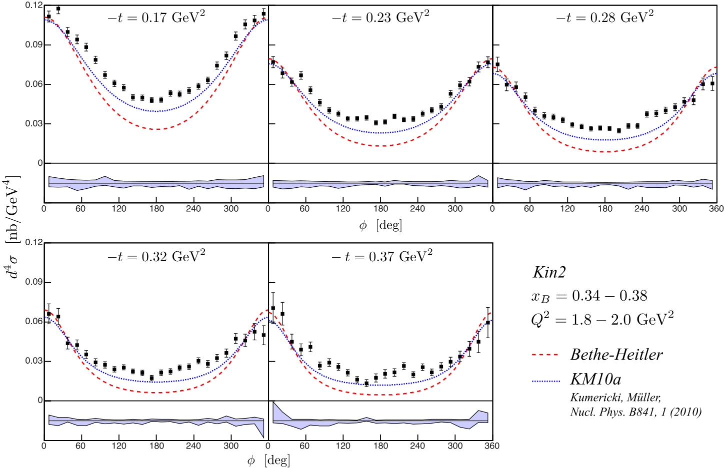

- KM10a: global fit to HERA x-sec & HERMES + CLAS spin asymmetries

Kumericki and Mueller (2010)

DVCS cross sections: kinematical power corrections

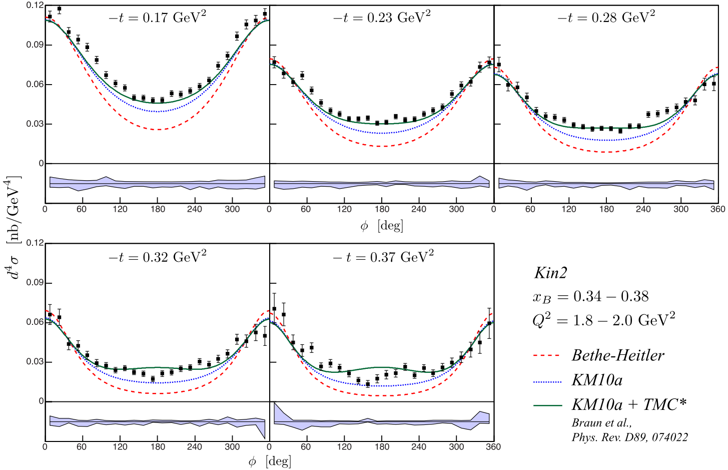

- KM10a: global fit to HERA x-sec & HERMES + CLAS spin asymmetries

  Kumericki and Mueller (2010)

- Target-mass corrections (TMC): $\sim \mathcal{O}(M^2/Q^2)$ and $\sim \mathcal{O}(t/Q^2)$

  Braun, Manashov, Mueller and Pirnay (2014)

Rosenbluth-like separation of the DVCS cross section

$$\sigma(ep \to ep\gamma) = \underbrace{|BH|^2}_{\text{Known to} \sim 1\%} + \underbrace{\mathcal{I}(BH \cdot DVCS)}_{\text{Linear combination of GPDs}} + \underbrace{|DVCS|^2}_{\text{Bilinear combination of GPDs}}$$

$$\mathcal{I} \propto 1/y^3 = (k/\nu)^3,$$

$$\left|\mathcal{T}^{DVCS}\right|^2 \propto 1/y^2 = (k/\nu)^2$$

BKM-2010 – at leading twist → 7 independent GPD terms:

$$\left\{\Re\text{e}, \Im\text{m}\left[\mathcal{C}^{\mathcal{I}}, \mathcal{C}^{\mathcal{I},V}, \mathcal{C}^{\mathcal{I},A}\right](\mathcal{F})\right\}, \quad \text{and} \quad \mathcal{C}^{DVCS}(\mathcal{F}, \mathcal{F}*).$$

φ-dependence provides 5 independent observables:

$$\sim 1, \sim \cos\varphi, \sim \sin\varphi, \sim \cos(2\varphi), \sim \sin(2\varphi)$$

The measurement of the cross section at two or more beam energies for exactly the same Q^2, x_B, t kinematics, provides the additional information in order to extract all leading twist observables independently.

E07-007: DVCS beam-energy dependence

- Cross section measured at 2 beam energies and constant Q^2, x_B, t

$E = 4.5$ GeV $E = 5.6$ GeV

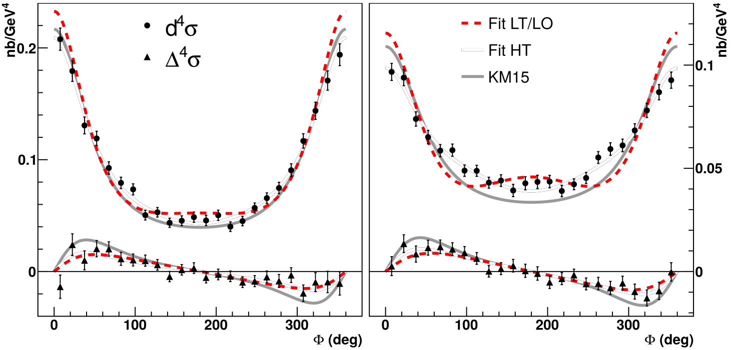

- Leading-twist and LO simultaneous fit of both beam energies (dashed line) does not reproduce the data

Light-cone axis in the (q,q') plane (Braun et al.): $\mathbb{H}_{++}$, $\widetilde{\mathbb{H}}_{++}$, $\mathbb{E}_{++}$, $\widetilde{\mathbb{E}}_{++}$

Beyond Leading Order (LO) and Leading Twist (LT)

Two fit-scenarios:

Light-cone axis in the (q, q') plane (Braun et al.)

LO/LT + HT

$\mathbb{H}_{++}$, $\widetilde{\mathbb{H}}_{++}$, $\mathbb{H}_{0+}$, $\widetilde{\mathbb{H}}_{0+}$

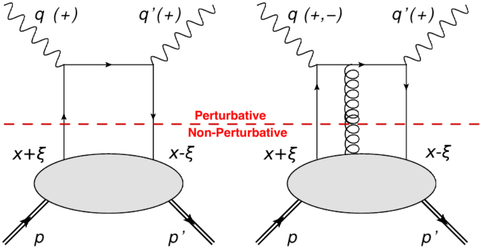

LO/LT + NLO

$\mathbb{H}_{++}$, $\widetilde{\mathbb{H}}_{++}$, $\mathbb{H}_{-+}$, $\widetilde{\mathbb{H}}_{-+}$

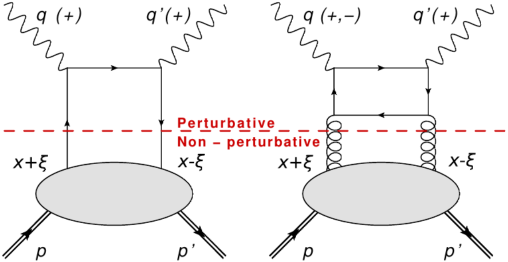

E07-007: DVCS beam-energy dependence

- Cross section measured at 2 beam energies and constant Q^2, x_B, t

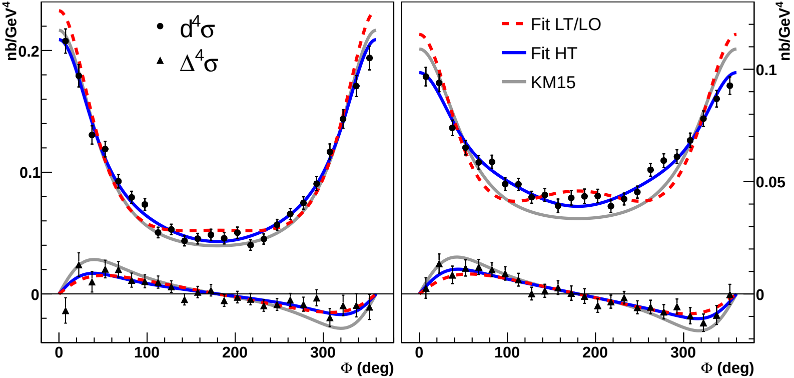

- Leading-twist and LO simultaneous fit of both beam energies (dashed line) does not reproduce the data
- Including either NLO or higher-twist effects (dark solid line) satisfactorily reproduce the angular dependence

DVCS^2 and $\mathcal{I}$ (DVCS·BH) separation

DVCS^2 and $\mathcal{I}$ (DVCS·BH) separated in NLO and higher-twist scenarios

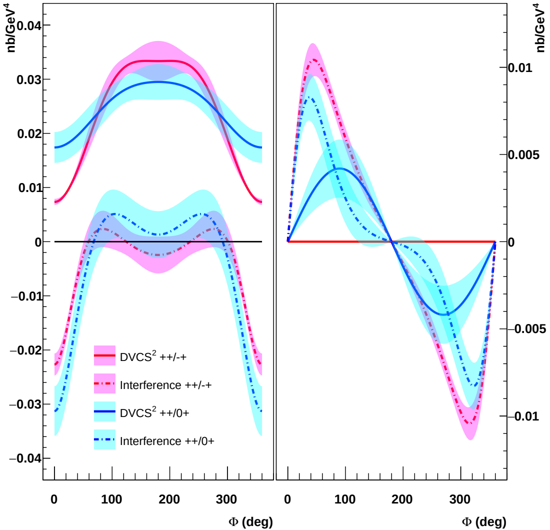

- DVCS^2 & $\mathcal{I}$ significantly different in each scenario
- Sizeable DVCS^2 contribution in the higher-twist scenario in the helicity-dependent cross section

Nature Commun. 8, 1408 (2017)

π^0 electroproduction ($ep \to ep\pi^0$)

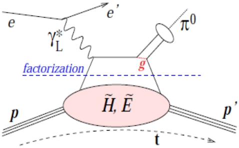

At leading twist:

$$\frac{d\sigma_L}{dt} = \frac{1}{2}\Gamma \sum_{h_N, h_{N'}} |\mathcal{M}^L(\lambda_M = 0, h'_N, h_N)|^2 \propto \frac{1}{Q^6} \qquad \sigma_T \propto \frac{1}{Q^8}$$

$$\mathcal{M}^L \propto \left[\int_0^1 dz \frac{\phi_\pi(z)}{z}\right] \int_{-1}^{1} dx \left[\frac{1}{x-\xi} + \frac{1}{x+\xi}\right] \times \left\{\Gamma_1 \tilde{H}_{\pi^0} + \Gamma_2 \tilde{E}_{\pi^0}\right\}$$

Different quark weights: flavor separation of GPDs

$$|\pi^0\rangle = \frac{1}{\sqrt{2}}\{|u\bar{u}\rangle - |d\bar{d}\rangle\} \qquad \tilde{H}_{\pi^0} = \frac{1}{\sqrt{2}}\left\{\frac{2}{3}\tilde{H}^u + \frac{1}{3}\tilde{H}^d\right\}$$

$$|p\rangle = |uud\rangle \qquad H_{DVCS} = \frac{4}{9}H^u + \frac{1}{9}H^d$$

Exclusive π^0 electroproduction cross-sections – Hall A

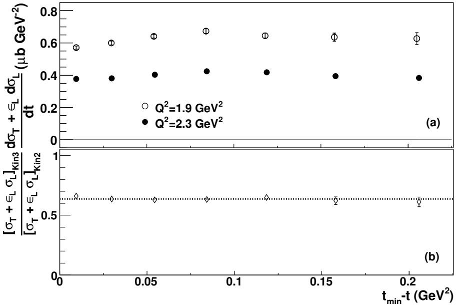

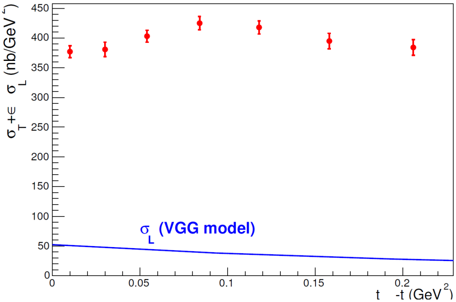

- $\sigma_T + \epsilon_L \sigma_L \sim Q^{-5}$
  (similar to $\sigma_T(ep \to ep\pi^+)$ measured in Hall C)
- GPDs predict $\sigma_L \sim Q^{-6}$
- σ_T likely to dominate at these Q^2,
  but L/T separation necessary ($\to$ new experiment...)

E. Fuchey et al., Phys. Rev. C83 (2011), 025125

Rosenbluth separation

$$\frac{d^4\sigma}{dQ^2 dx_B dt d\phi} = \frac{1}{2\pi}\Gamma(Q^2, x_B, E)\left[\frac{d\sigma_T}{dt} + \epsilon\frac{d\sigma_L}{dt} + \sqrt{2\epsilon(1+\epsilon)}\frac{d\sigma_{TL}}{dt}\cos\phi + \epsilon\frac{d\sigma_{TT}}{dt}\cos\right.$$

Kinematics

Setting	Q^2 (GeV^2)	x_B	E^{beam} (GeV)	ϵ
Kin1	1.50	0.36	3.355	0.52
			5.55	0.84
Kin2	1.75	0.36	4.455	0.65
			5.55	0.79
Kin3	2.00	0.36	4.455	0.53
			5.55	0.72

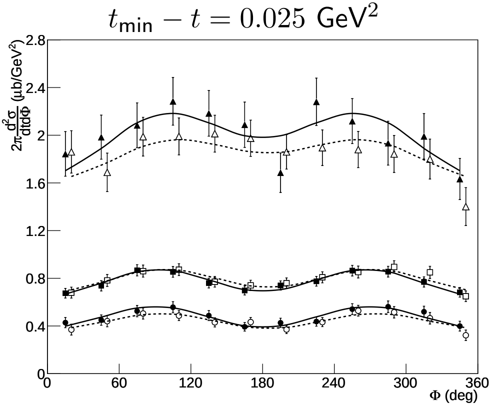

π^0 separated response functions

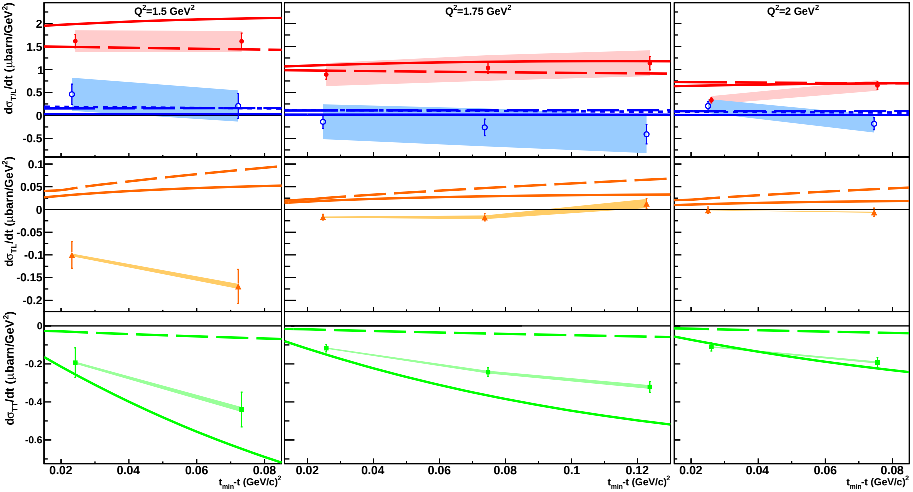

Goloskokov, Kroll (2011)

Goldstein, Hernandez, Liuti (2011)

Vanderhaeghen, Guichon, Guidal (1999)

arXiv:1608.01003

π^0 L/T separated cross section

- Cross section largely dominated by transverse component

  $\rightarrow$ far from asymptotic prediction of QCD

- Fair agreement with models using modified factorization approach

  $\rightarrow$ potential access to transversity GPDs

- Indications of small longitudinal response through non-zero σ_{LT}

E08-025: DVCS and π^0 off quasi-free neutrons

- LD_2 as a target
- Quasi-free p evts subtracted using the (normalized) data from E07-007
- Concurrent running: switching LD2/LD2 $\rightarrow$ minimize uncertainties

$$D(e, e\,\pi^0)X - p(e, e\,\pi^0)p = n(e, e\,\pi^0)n + d(e, e\,\pi^0)d$$

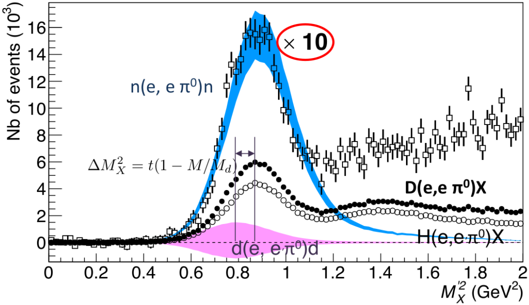

The average momentum transfer to the target is much larger than the np relative momentum, justifying this **impulse approximation**

π^0 electroproduction cross section off the neutron

- Cross section off coherent d found negligeable within uncertainties
- Very low E_{beam} dependence of the n cross section $\rightarrow$ dominance of σ_T

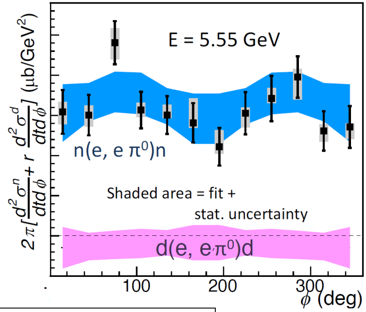

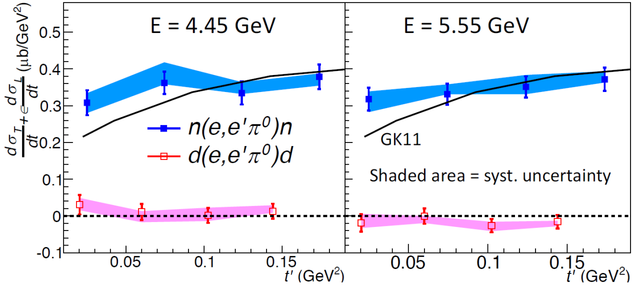

Separated π^0 cross section off the neutron

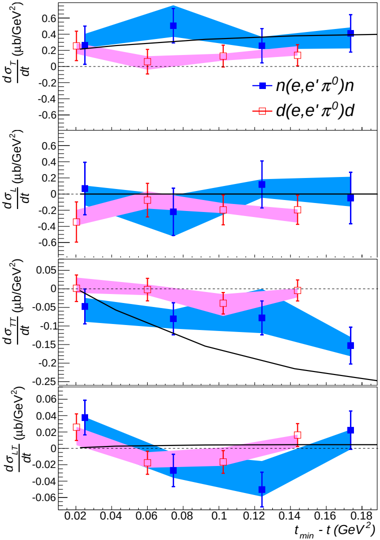

M. Mazouz et al, Phys.Rev.Lett. 118 (2017)

In the modified factorization approach (KG):

- $d\sigma_T \propto \left[\left(1-\xi^2\right)\left|\langle H_T\rangle\right|^2 - \frac{t'}{8M^2}\left|\langle \bar{E}_T\rangle\right|^2\right]$
- $d\sigma_{TT} \propto \frac{t'}{8M^2}\left|\langle \bar{E}_T\rangle\right|^2$

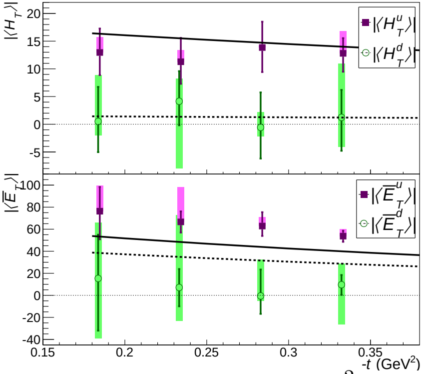

$$\left|\langle H_T^{p,n}\rangle\right|^2 = \frac{1}{2}\left|\frac{2}{3}\left\langle H_T^{u,d}\right\rangle + \frac{1}{3}\left\langle H_T^{d,u}\right\rangle\right|^2$$

E12-06-114: JLab Hall A at 11 GeV

JLab12 with 3, 4, 5 pass beam

(6.6, 8.8, 11.0 GeV beam energy)

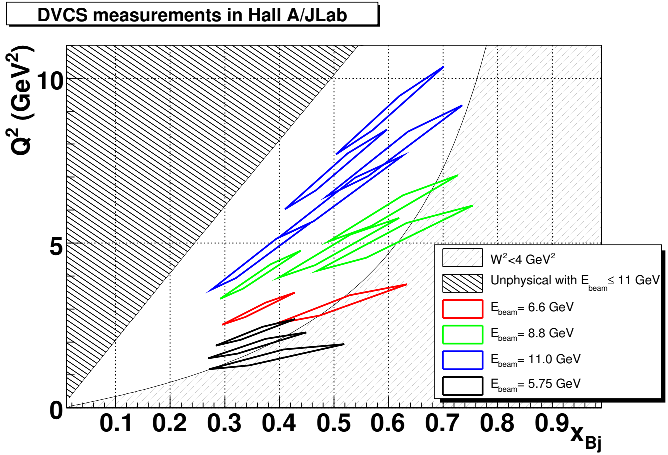

88 days

250k events/setting

1 year of operations in JLab/Hall A

Cumulated statistics

Scaling tests of the DVCS cross section

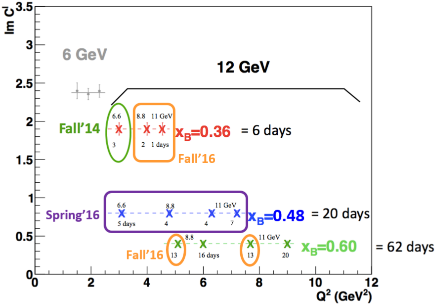

Period	Kinematic	Q^2	x_B	% target Charge
F '14	361	3.20	0.36	100.0
F '16	362	3.60	0.36	100.0
F '16	363	4.47	0.36	100.0
Sp '16	481	2.7	0.48	100.0
Sp '16	482	4.37	0.48	56.6
Sp '16	483	5.33	0.48	76.4
Sp '16	484	6.90	0.48	53.0
F '16	601	5.54	0.60	100.0
~~F '16~~	~~602~~	~~6.10~~	~~0.60~~	~~0.0~~
F '16	603	8.40	0.60	100.0
~~F '16~~	~~604~~	~~9.00~~	~~0.60~~	~~0.0~~

F– Fall Sp– Spring Q^2 – in GeV^2

~50% of allocated 100 PAC days from Fall 2014, Spring 2016, and Fall 2016

Analysis status

Beam Studies
- ✔ Beam energy measurement
- ✔ Polarization measurement
- ✔ Raster calibration
- ✔ BCM/BPM calibration

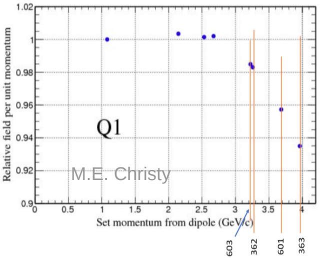

High Resolution Spectrometer
- ✔ Trigger Efficiency
- ✔ Particle Identification
- ✔ Optics calibration
- ✔ Tracking Efficiency
- ✔ Acceptance Studies
- ✔ DIS x-section

Calorimeter
- ✔ Coincidence time correction
- ✔ Waveform analysis
- ✔ Elastic and π^0 calibration
- ✔ π^0 electroproduction (in progress)

✔DVCS Simulation

Q1 Status
Fall 2014 : Old Q1 at full field
Spring 2016: Maximum current was limited to 2.8 GeV setting (detuned)
Fall 2016: Q1 saturated

8

B. Karki - Hall A Coll. Meet. (Jan'18)

Calorimeter resolution

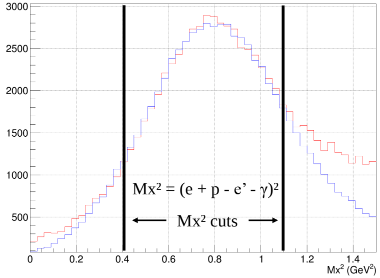

Normalized Geant4 smeared missing mass
VS
data

- Geant4 reconstructed photons energy smeared with Gaussian(mean,sigma).
- (mean,sigma) computed by χ^2 minimization :

$$\chi^2 = \sum \frac{data\_Mx^2 - geant4\_Mx^2}{\sigma^2(data\_Mx^2)}$$

- (mean,sigma) dependence against position in calorimeter

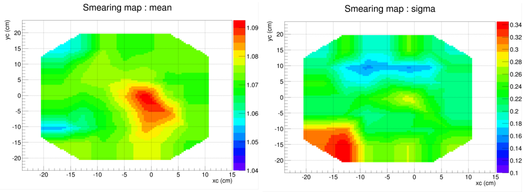

F. Georges

E12-13-010: DVCS in Hall C

- HMS ($p < 7.3 GeV$): scattered electron
- $PbWO_4$ calorimeter: γ/π^0 detection
- Sweeping magnet

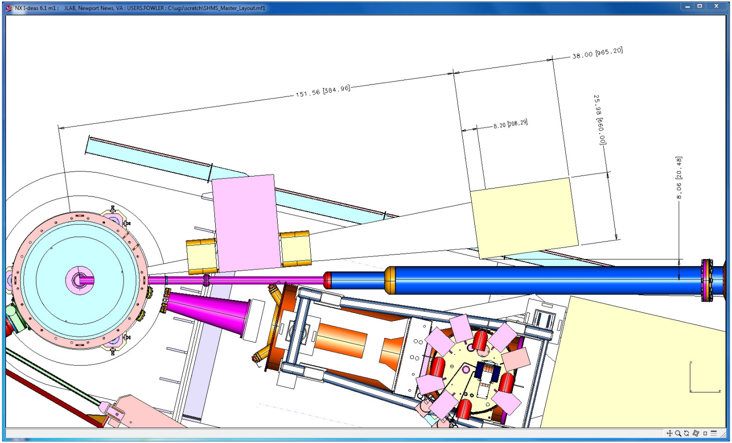

E12-13-010: beam energy separation in Hall C

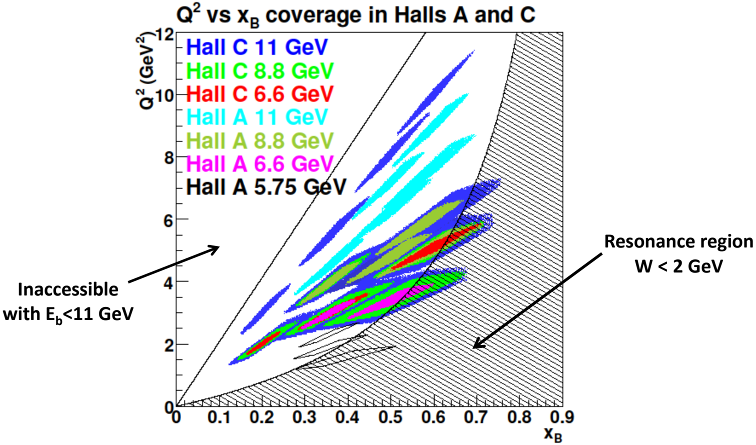

Approved by the PAC, possible running in $\gtrsim 2020$

Projections

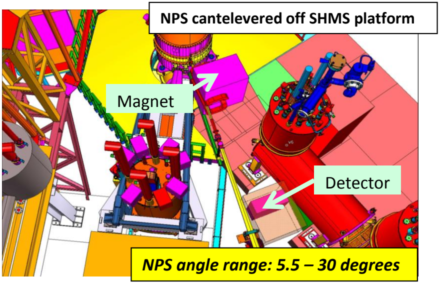

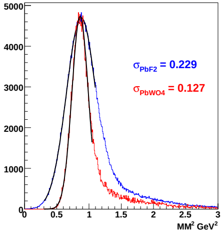

- $PbF_2 \rightarrow PbWO_4$
- Improved E resolution wrt Hall A

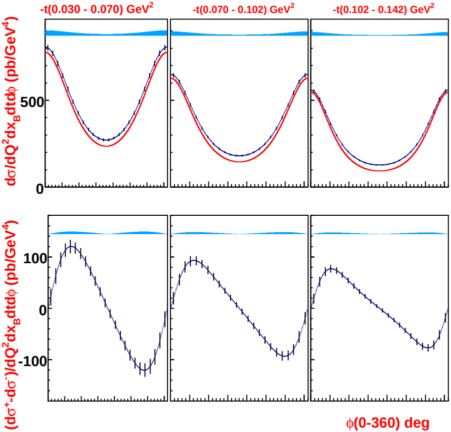

NPS construction

NPS Project Status

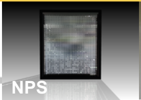

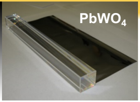

Four fully approved experiments, one conditionally, one PAC46 proposal supported by NSF MRI PHY-1530874 (CUA, OU, ODU), international (IPN-Orsay, Glasgow, Yerevan), JLab

- Magnet: corrector coil, main coil and yoke steel at JLab, assembly has started, testing and field map next

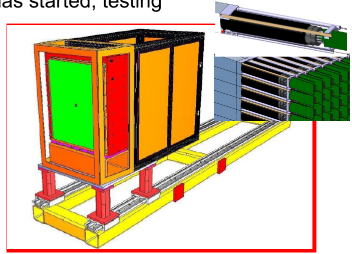

- PMT and HV bases: design drawings final, prototyping, procurement started, first articles received
- Frame and integrated systems: concepts and initial design complete, detailed drawings to be presented later this year, prototype tests ongoing

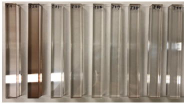

NPS crystal prototype and irradiation studies

- Crystals: 460 crystals procured from SICCAS in 2017, 400 SICCAS + 100 CRYTUR procurement ongoing in 2018, full crystal testing facilities established at CUA and IPN-Orsay, chemical analysis and crystal growth in collaboration with Vitreous State Laboratory @ CUA, synergy with EIC crystal calorimeter R&D.

Summary

- Hall A & C GPD program is dedicated to precision measurements of DVCS and DVMP:
  - Exploit the high luminosity and excellent detector capabilities of JLab12
  - Understand the contribution of higher order and higher twist
- Large and accurate set of data is now available
  - Dominance of leading twist, but...
  - Necessity of higher twist corrections to explain high precision data
- Compeling GPD program in the future at Jefferson Lab 12 GeV in all 3 electron Hall A, B & C.

Back-up

DVCS process: leading twist ambiguity

- DVCS defines a preferred axis: light-cone axis
- At finite Q^2 and non-zero t, there is an ambiguity:
  1. Belitsky et al. ("BKM", 2002–2010): light-cone axis in plane (q,P)
  2. Braun et al. ("BMP", 2014): light-cone axis in plane (q,q')
     easi*er* to account for kin. corrections $\sim \mathcal{O}(M^2/Q^2)$, $\sim \mathcal{O}(t/Q^2)$

$$\left.\begin{array}{ll} \mathcal{F}_{++} = & \mathbb{F}_{++} + \frac{\chi}{2}\left[\mathbb{F}_{++} + \mathbb{F}_{-+}\right] - \chi_0 \mathbb{F}_{0+} \\ \mathcal{F}_{-+} = & \mathbb{F}_{-+} + \frac{\chi}{2}\left[\mathbb{F}_{++} + \mathbb{F}_{-+}\right] - \chi_0 \mathbb{F}_{0+} \\ \mathcal{F}_{0+} = & -(1+\chi)\mathbb{F}_{0+} + \chi_0\left[\mathbb{F}_{++} + \mathbb{F}_{-+}\right] \end{array}\right\} \xrightarrow[\mathbb{F}_{0+}=0]{\mathbb{F}_{-+}=0} \left\{\begin{array}{ll} \mathcal{F}_{++} & = (1+\frac{\chi}{2})\mathbb{F}_{++} \\ \mathcal{F}_{-+} & = \frac{\chi}{2}\mathbb{F}_{++} \\ \mathcal{F}_{0+} & = \chi_0 \mathbb{F}_{++} \end{array}\right.$$

(eg. $\chi_0 = 0.25$, $\chi = 0.06$ for $Q^2 = 2$ GeV^2, $x_B = 0.36$, $t = -0.24$ GeV^2)